ELSEVIER

Journal of Fluids and Structures 18 (2003) 759–770

JOURNAL OF FLUIDS AND STRUCTURES

www.elsevier.nl/locate/jnlabr/yjfls

Characteristics of aerodynamic sound sources generated by coiled wires in a uniform air-flow

H. Matsumoto*, K. Nishida, K. Saitoh

Department of Mechanical Systems Engineering, Muroran Institute of Technology, 27-1 Mizumoto-Cho, Muroran-City Hokkaido 050-8585, Japan

Received 24 February 2003; accepted 14 August 2003

Abstract

This study deals experimentally with aerodynamic sounds generated by coiled wires in a uniform air-flow. The coiled wire is a model of the hair dryer's heater. In the experiment, the effects of the coil diameter D, wire diameter d and coil spacing s of the coiled wire on the aerodynamic sound have been clarified. The results of frequency analyses of the aerodynamic sounds show that an Aeolian sound is generated by the coiled wire, when s/d is larger than 1. Also the peak frequencies of Aeolian sounds generated by the coiled wires are higher than the ones generated by a straight cylinder having the same diameter d. To clarify the characteristics of the aerodynamic sound sources, the directivity of the aerodynamic sound generated by the coiled wire has been examined, and the coherent function between the velocity fluctuation around the coiled wire and the aerodynamic sound has been calculated. Moreover, the *band overall value of coherent output power* between the sound and the velocity fluctuations has been calculated. This method has clarified the sound source region of the Aeolian sound generated by the coiled wire. These results show that the Aeolian sound is generated by the arc part of the coiled wire, which is located in the upstream side of the air-flow.

1. Introduction

The sound environment in our daily life has become uncomfortable due to the many kinds of noise. For example, in the case of a hair dryer, aerodynamic noise and motor noise are generated. If the mechanism of these noise generations is clarified, it would become possible to take effective countermeasures for decreasing such noise. In particular, it is difficult to find the aerodynamic noise source regions. In the studies of this kind done so far, the straight round bar has been chiefly chosen as the subject of each study (e.g., Fujita et al., 1996, 1997; Iida et al., 1998; Mochizuki et al., 1994). However, in practical structures, not only straight round bars but also bent round bars have been widely used.

In this study, we focus on the aerodynamic sound generated by the coiled wire. The coiled wire is used in the hair dryer as the heater. The purpose of this research is to clarify the characteristics of the aerodynamic sound generated by the coiled wire, and to find the wake region that has strong correlation with the Aeolian sound by examining the coherence function between the Aeolian sound and the velocity fluctuation in the wake behind the coiled wire.

2. Experimental equipment

The experimental equipment is shown in Fig. 1. The wind tunnel is an open type with a rectangular nozzle of 100 mm × 100 mm. A precision sound level meter and a hot-wire anemometer are used for measuring the aerodynamic

*Corresponding author.
E-mail address: h_matsu@mmm.muroran-it.ac.jp (H. Matsumoto).

0889-9746/$ - see front matter
doi:10.1016/j.jfluidstructs.2003.08.017

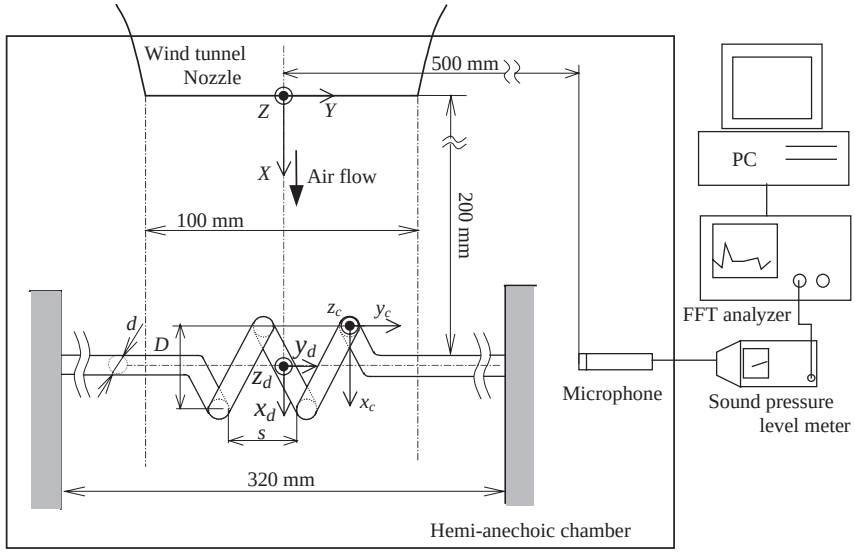

Fig. 1. Experimental equipment.

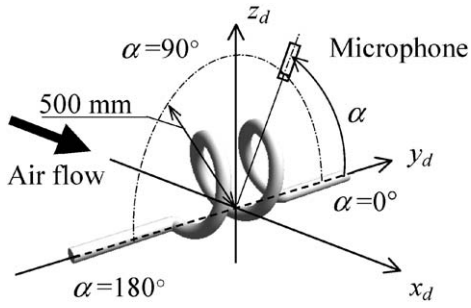

Fig. 2. Definition of coordinates for measurement of directivity patterns.

sound and the velocity fluctuations, respectively. The air-flow velocity is determined by the static pressure differential between the inlet and outlet of the nozzle. The flow in the test-section (at $X = 200$ mm) has a turbulence intensity of 0.8% in the section of 70 mm × 70 mm and a velocity profile uniformity of better than 95% in the section of 80 mm × 80 mm. The microphone is installed in the $y_d - z_d$ plane at a position of $X = 200$ mm. Fig. 2 shows the coordinate system for measuring the directivity pattern. The position of microphone is indicated by the angle α. The tungsten single sensor hot wire probe (5 μm dia., 1 mm long) is attached to the traverse device by which the velocity fluctuations can be measured at an arbitrary location in the wake behind the coiled wire. All the experiments are performed in an hemi-anechoic chamber. In Fig. 1, D is coil diameter, d is wire diameter and s is coil spacing; the total number of turns is 2. In the experiment, the effects of D, d and s on the aerodynamic sound are investigated.

The coiled wire is set up in the horizontal plane containing the center of the nozzle section. Moreover, the axis of coil is located at the position of $X = 200$ mm and parallels the Y-axis. The diameter of the wire, d, is 3 or 4 mm. The mean velocity of air-flow, U, used is between 20 and 40 m/s.

3. Measurement method

3.1. Background noise

In this study, background noise (BGN) is defined as the noise generated by the air-flow. The coiled wire model has a helical coil part and straight cylinder parts. Thus, the aerodynamic sound generated by this model contains the sound

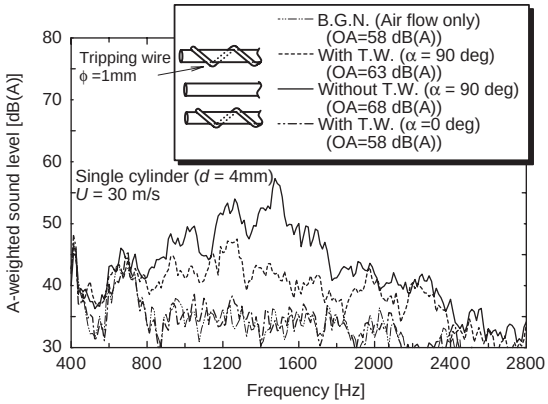

Fig. 3. Effect of TW on spectra of aerodynamic sounds generated by cylinders. ($U = 30\,\mathrm{m/s}$, $d = 4\,\mathrm{mm}$).

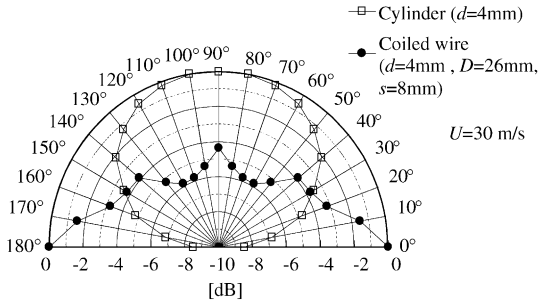

Fig. 4. Directivity patterns of aerodynamic sounds generated by the coiled wire and the single cylinder.

generated by the helical coil part and that generated by the straight cylinder parts. In order to reduce the noise generated by the straight parts, tripping wires (TW) are attached on the straight parts. The diameter of the TW is 1 mm, and the pitch of wires is 10 mm. Fig. 3 shows the effect of the TW on the spectrum of aerodynamic noise generated by the single cylinder. The A-weighting precision sound pressure level meter measures these sound levels. The position of microphone is $\alpha = 90^\circ$. The cylinder without the TW generates the Aeolian sound with a peak at 1475 Hz. However, the aerodynamic sound generated by the cylinder with the TW has no prominent peaks. An overall sound pressure level (OA) reduction of about 6 dB is obtained. These results show that the TW is effective to reduce the aerodynamic sound generated by the cylinder. Moreover, when the microphone is positioned at $\alpha = 0^\circ$, the spectrum of aerodynamic noise generated by the cylinder with TW nearly equals the spectrum of BGN. These results show that the aerodynamic noise generated by the straight cylinder parts can be neglected, when the microphone is positioned at $\alpha = 0^\circ$ and 180°.

3.2. Determination of the microphone position

The aerodynamic sound generated by the coiled wire has a unique directivity pattern. Fig. 4 shows the directivity patterns of the sound fields generated by the coiled wire and a single cylinder of the same diameter $d = 4$.

Each plot is normalized by its own maximum value of overall sound level. In the case of the single cylinder, the directivity pattern has a lobe along the $\alpha = 90^\circ$ axis, but the radiation energy of this sound source is very weak in the direction of the $\alpha = 0^\circ$ axis. However, in the case of coiled wire, the directivity pattern is more complicated and it has the principal lobe along the $\alpha = 0$–180° axis. For this reason, the measurements were carried out with the microphone located at $\alpha = 0^\circ$.

3.3. Measurement of the band overall value of COP

The coherent output power (COP) (Bendat and Piersol, 1980) is used for the evaluation of the correlation strength between the velocity fluctuation of the wake behind the coiled wire and the generated aerodynamic sound.

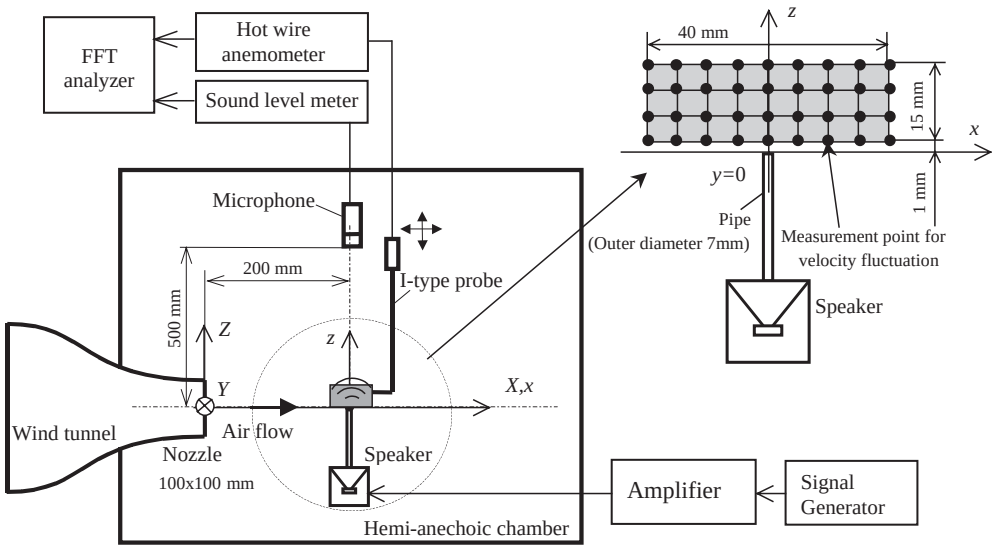

Fig. 5. Experimental equipment for determination of ψ_{vb}.

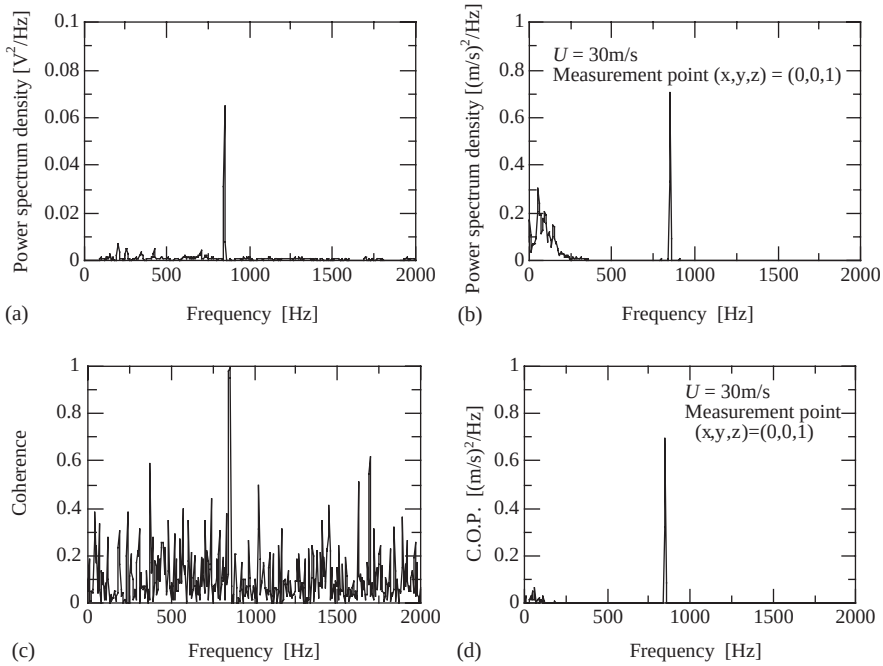

Fig. 6. (a) Power spectrum of the sound at the microphone position $(X, Y, Z) = (200, 0, 500)$. (b) Power spectrum of the velocity fluctuations at the position $(x, y, z) = (0, 0, 1)$. (c) Coherence function. (d) COP (= Coherence function × Power spectrum of velocity fluctuation).

The coherence function is calculated by

$$\gamma_{xy}^2(f) = \frac{|G_{xy}(f)|^2}{G_{xx}(f)G_{yy}(f)}, \quad 0 \leqslant \gamma_{xy}^2(f) \leqslant 1, \tag{1}$$

where G_{xx} and G_{xy} are the power spectral density function of the sound and the sound/velocity fluctuation cross-spectral density function, respectively. G_{yy} is power spectral density function of the velocity fluctuation of the wake.

G_{xx}, G_{xy} are measured quantities. The coherent output power spectrum (COP) is calculated by

$$G_{vv}(f) = \gamma_{xy}^2(f) G_{yy}(f). \tag{2}$$

COP is the power spectrum of the velocity fluctuations that has a correlation with the aerodynamic sound generated by the coiled wire.

Furthermore, the value of COP is integrated over a specific frequency range in order to clarify the strength of the correlation between the aerodynamic sound in the specific frequency range and the velocity fluctuation of the wake behind the coiled wire. The integrated value is called the band overall value of COP. The band overall value of COP is calculated by

$$\psi_{v(f_l - f_u)} = \int_{f_l}^{f_u} G_{vv}(f)\,\mathrm{d}f. \tag{3}$$

Here f_l and f_u are the lower and the upper frequencies in the integrated frequency range. The distribution of the normalized value of $\psi_{nv}(f_l - f_u)$ shows the wake region which has strong correlation with the specific frequency range for the aerodynamic sound generated by the coiled wire. The normalized value is calculated by

$$\psi_{nv(f_l - f_u)} = \frac{\psi_{v(f_l - f_u)}}{\psi_{bv}}, \tag{4}$$

where ψ_{bv} denotes the band overall value of COP which is obtained between a pure tone generated by a speaker and the velocity fluctuation above the sound source.

In the experiment, the microphone at a fixed position measures the aerodynamic sound, and the velocity fluctuation of the wake is systematically measured at many points by the hot-wire anemometer. In order to obtain ψ_{bv}, we use a speaker with a pipe as the sound source in air-flow. Fig. 5 shows the experimental equipment and a measurement plane. A pure tone is radiated from the pipe in the air-flow at 30 m/s. The frequency of the pure tone is 850 Hz. The measurements are performed on a 5 mm grid in the $X-Z$ plane. Fig. 6 is an example of the experimental results. Fig. 6(a) shows the power spectrum of the sound pressure measured by the microphone, and Fig. 6(b) shows the velocity fluctuation, respectively. The measurement of the velocity fluctuations is made at the position $(x, y, z) = (0, 0, 1)$. Fig. 6(c) shows the coherence function between the sound pressure and the velocity fluctuations; Fig. 6(d) shows the COP spectrum at the position $(x, y, z) = (0, 0, 1)$. In Figs. 6(a) and (b), the spectra have a peak at the same frequency of 850 Hz. Thus, the coherence function has the value of 1 at 850 Hz. Therefore, the velocity fluctuations at this measurement point and the radiated sound have a strong correlation at 850 Hz and the COP has a peak at that frequency.

Fig. 7 is the distribution of $\psi_{v(850)} = G_{vv(850)}$ around the sound source in the air-flow. The results show that $\psi_{v(850)}$ has a maximum value at the position $(x, y, z) = (0, 0, 1)$. Assuming that the top of the pipe is the sound source, Fig. 7 shows that the sound source of pure tone is determined by this method. In addition, we denote $\psi_{v(850)}$ measured at the position $(x, y, z) = (0, 0, 1)$ as ψ_{bv}. The COP is used for the evaluation of the correlation strength between the velocity fluctuation of the wake behind the coiled wire and the generated aerodynamic sound.

4. Experimental results

4.1. Characteristics of the aerodynamic sound generated by the coiled wires

The frequency characteristics of the aerodynamic sound generated by the coiled wires have been examined for various values of s and D. An example of the frequency characteristics of the aerodynamic sound generated by the coiled wire ($D = 26$ mm, $s = 8$ mm) is shown in Fig. 8. In this figure, the dotted line is the spectrum of Aeolian sound generated by the single cylinder of the same diameter $d = 4$ mm. The spectrum of the coiled wire has a prominent peak at 1600 Hz. This peak frequency is higher than the Aeolian sound generated by the single cylinder. Moreover, the overall sound level is larger than that of the single cylinder.

The effects of the coil spacing s on the frequency characteristics of the aerodynamic sound generated by the coiled wires are shown in Fig. 9. In the case of $s = 8$ mm, the frequency spectrum displays a prominent peak at 1600 Hz.

However, in the case of $s = 6$ mm, the peak sound level is smaller than that for $s = 8$ mm. The sound level of this peak becomes weaker as s decreases. In the case of $s = 2$ mm, the frequency spectrum has no prominent peak at 1600 Hz. In view of the present result, it seems that the prominent peak first appears in the spectra when the value s/d is between 1 and 1.5.

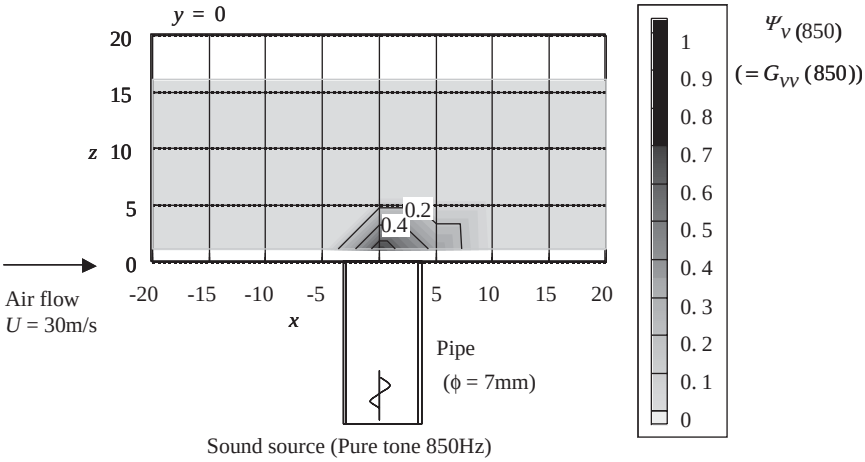

Fig. 7. Distribution of a band overall value of COP around a sound source.

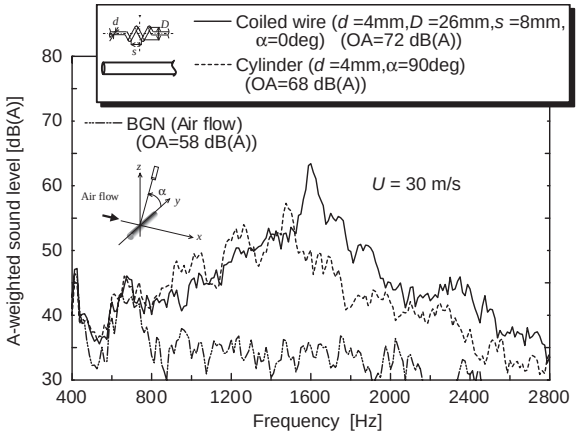

Fig. 8. Spectra of aerodynamic sound generated by the coiled wire ($U = 30$ m/s, $d = 4$ mm, $D = 26$ mm, $s = 8$ mm) and the single cylinder ($d = 4$ mm).

The effects of the coil diameter D on the frequency characteristics of the aerodynamic sound generated by the coiled wire are shown in Fig. 10. The coil spacing s is 8 mm ($s/d = 2$). In all cases, the spectra have a peak around 1600 Hz. Under these conditions, it can be considered that there is no effect of D on the peak frequency. Moreover, the sound levels of these peaks are independent of D.

The Strouhal number based on d is plotted in Fig. 11 as a function of Reynolds number. The Reynolds number is based on d. The coiled wire has a constant value of $s/d = 2$; i.e., in the case of $d = 3$ mm, s is 6 mm. Fig. 11 shows that the Strouhal number of coiled wires is about 0.22. This value is slightly higher than the Strouhal number of the single circular cylinder. However, when the Reynolds number is between 4255 and 11 347, the corresponding Strouhal number is approximately constant. Therefore, it is considered that this aerodynamic sound with the prominent peak can be called an Aeolian sound induced by the Karman vortex street.

4.2. The aerodynamic sound generated by the semicircular wire

In order to identify the source of vortex shedding, a semicircular wire model that is similar to the coiled wire is used. The semicircular wire is shown in Fig. 12. In the case of Type-A wire, the arc part is located at the upstream side of the flow, and in the case of Type-B wire, at the downstream side of the flow. The measuring microphone position is $\alpha = 90^\circ$, i.e., $(X, Y, Z) = (200, 0, 500)$. Fig. 13 shows the spectra of the aerodynamic sound generated by the semicircular wires. The semicircular wire has an outer diameter $D = 26$ mm, and a wire diameter $d = 4$ mm. In the case of Type-A wire, the

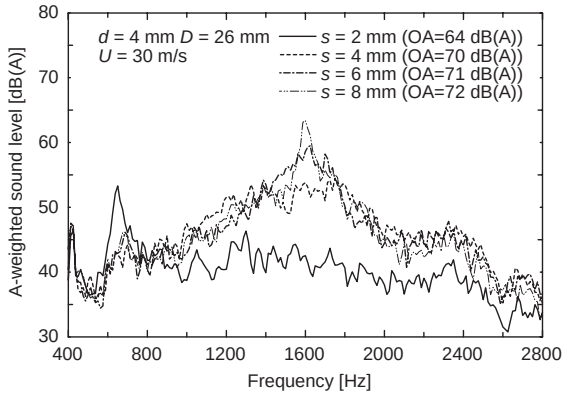

Fig. 9. Effect of the spacing between coils s on the aerodynamic sound generated by the coiled wire.

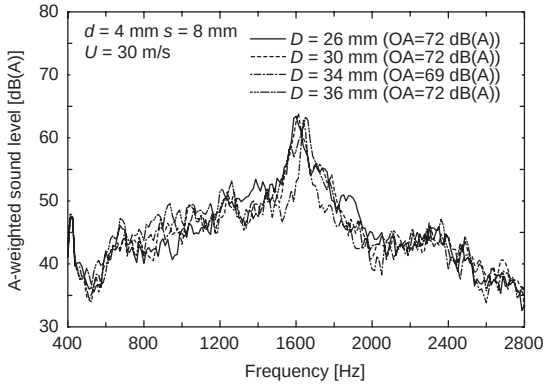

Fig. 10. Effect of the outer diameter D on the aerodynamic sound generated by the coiled wire.

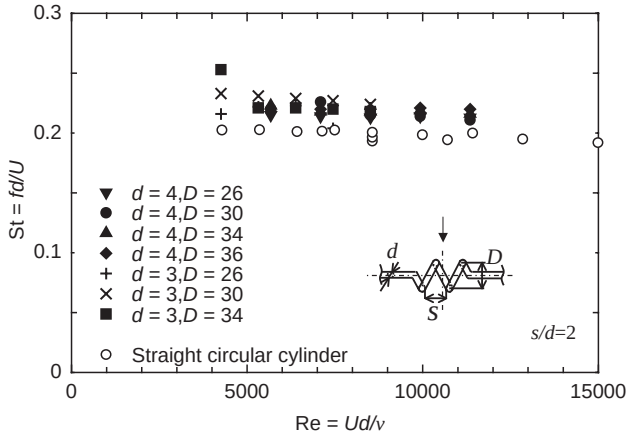

Fig. 11. Relationship between Strouhal number of the coiled wire ($s/d = 2$) and Reynolds number.

spectrum has a prominent peak at 1687 Hz; but in the case of Type-B wire, the peak disappeared and the overall sound level is rather small.

The distribution of the band overall value of COP is shown in Fig. 14. The semicircular wire used is of Type-A. The spectrum of aerodynamic sound generated by the Type-A semicircular wire has a peak at 1687 Hz. The $\psi_{nv(fl-fu)}$ is obtained over the frequency range of 1675–1775 Hz. This frequency range includes the peak frequency of the aerodynamic sound generated by the Type-A semicircular wire. In Fig. 14, the larger values of $\psi_{nv(1675-1775)}$ are clustered

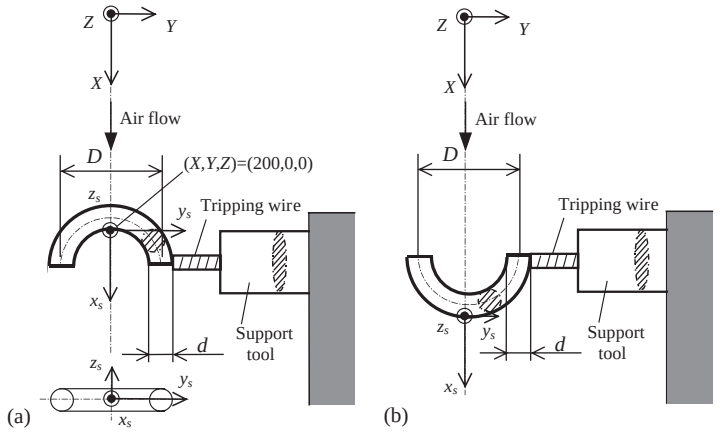

Fig. 12. Definition sketch of the semicircular wire. (a) Semicircular wire Type A and (b) Semicircular wire Type B.

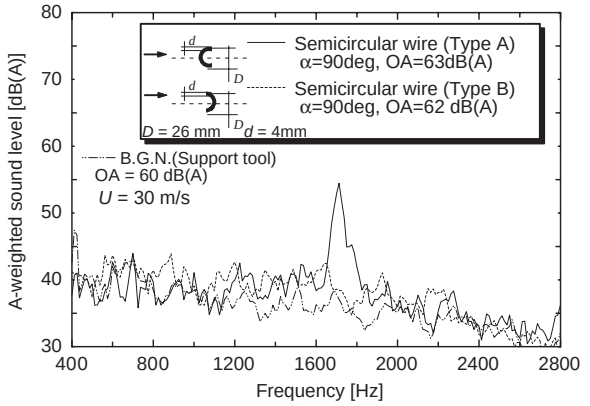

Fig. 13. Spectra of aerodynamic sound generated by semicircular wires.

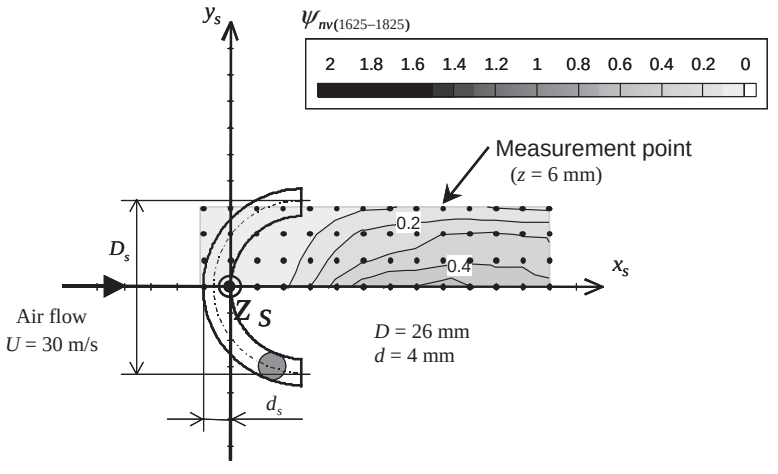

Fig. 14. Distribution of $\psi_{nv(1625-1825)}$ of the Type-A semicircular wire.

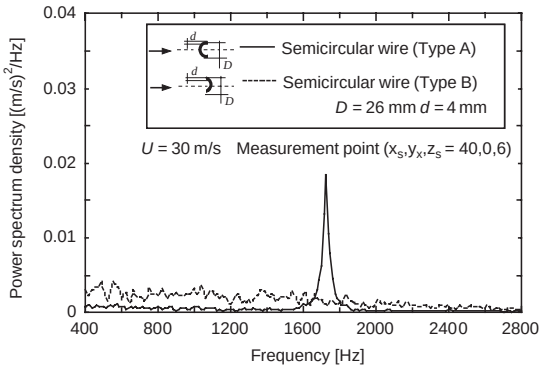

Fig. 15. Power spectra of velocity fluctuation behind a semicircular wire.

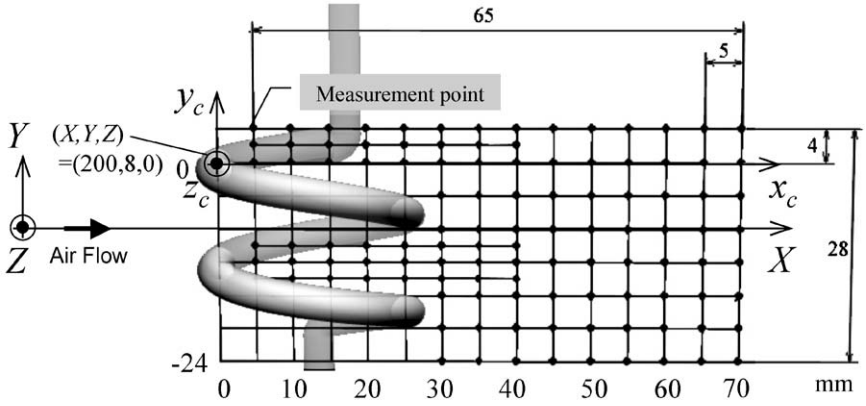

Fig. 16. Measurement plane for the velocity fluctuation by the hot-wire probe.

around the center-line referred to in the figure as the x_s-axis. Hence it is clear that the peak frequency of the Aeolian sound and the velocity fluctuations of the wake behind the cross-section on the x_s-axis of the semicircular wire (the center part of the semicircular wire) have a strong correlation in the region along the x_s-axis. It is considered that the flow that breaks away from the upper and the lower sides of the cross-section of the semicircular wire is fluctuating at the same frequency of the Aeolian sound. As a result, it has become clear that the Aeolian sound source is in the wake region behind the center part of the semicircular wire. Fig. 15 shows a comparison between the spectra of velocity fluctuations measured behind the semicircular wires Type-A and Type-B. Both measurement positions are $(x_s, y_s, z_s) = (40, 0, 6)$. The spectrum for Type-A wire has a prominent peak at 1687 Hz, which is the same as the peak frequency of the sound spectrum. However, the spectrum for Type-B wire has no prominent peaks and is similar to a spectrum curve for random noise. Therefore, the wake of Type-A wire has periodic fluctuations, but the wake of Type-B wire is a turbulent flow. Thus, in the case of coiled wire, it is possible that the Aeolian sound is generated by the wake of the upstream side of the coil.

4.3. The distribution of ψ_{nv} of the coiled wire

In order to identify the location of sound sources of the coiled wire, the distribution of the band overall value of COP has been measured. The measurement plane for the distribution of ψ_{nv} is defined as Fig. 16. The measurement plane is an $X - Y$ plane located at $Z = 0$ (containing the axis of coil). On the basis of the above experimental results, it is considered that this plane contains the larger values of ψ_{nv}.

The distribution of ψ_{nv} is shown in Fig. 17. The top figure shows a two-dimensional view of the distribution of ψ_{nv} and the bottom figure shows a three-dimensional view. The coiled wire used has the coil diameter $D = 26$ mm, wire diameter $d = 4$ mm and coil spacing $s = 8$ mm. The spectrum of aerodynamic sound generated by this coiled wire has been shown in Fig. 8. The peak frequency of the Aeolian sound is 1600 Hz. In Fig. 17, the values of $\psi_{nv}(f_l - f_u)$ have

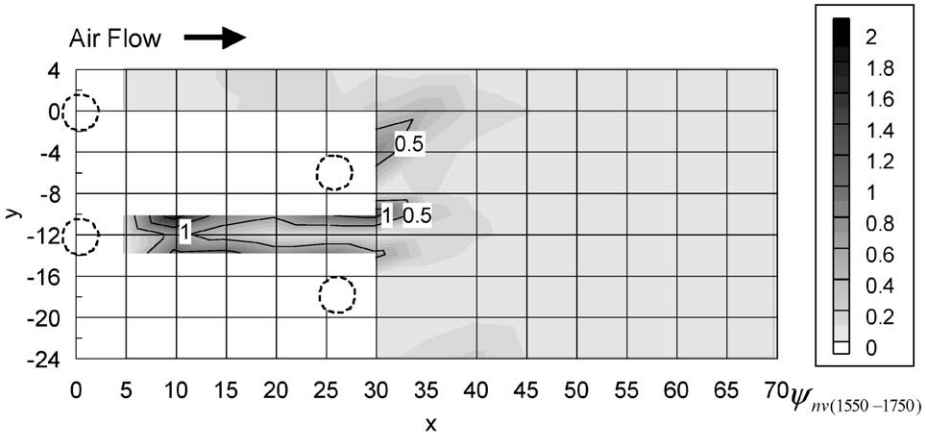

(a) 2-D view

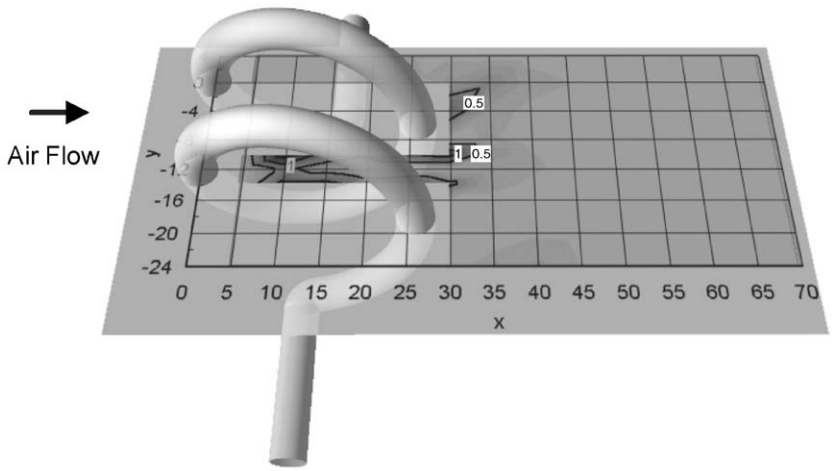

(b) 3-D view

Fig. 17. Distribution of the band overall value of COP ($\psi_{nv(1550-1750)}$) of the coiled wire.

been obtained over the frequency range of 1550–1750 Hz. The larger values of $\psi_{nv(1550-1750)}$ are clustered along the lines $y = -10$, -14 mm; but in the wake regions of downstream sides of coiled wire ($x > 30$ mm), the values of $\psi_{nv(1550-1750)}$ are small.

Therefore, the aerodynamic sound generated by the coiled wire is dominated by the vortex shedding from the upstream side of the coil. Also, we considered that the vortex shedding from the upstream side of the coil interacts with the downstream side of it, and then, the vortex is collapsed by the wake of downstream side of the coil. Figs. 18(a)–(d) are examples of power spectra of velocity fluctuations in the wake of the downstream side of the coil. The measurements are performed within the region between $x = 25$ mm and 40 mm in 5 mm intervals along the line of $y = -10$ mm.

In Fig. 18(a), the power spectrum of velocity fluctuations has the peak at 1600 Hz that corresponds to the peak frequency of the sound. However, the peak becomes weaker when the measurement point is at $x = 35$ (Fig. 18(c)). In Fig. 18(d), there is no peak at 1600 Hz, and this power spectrum has a larger value in the broad frequency range. At this measurement position (40,−10,0), the velocity fluctuation becomes disorganized. From these results we confirmed that the vortex collapsed in the wake behind the downstream sides of the coiled wire.

The configuration of the center portions of upstream and downstream coil wires resembles a staggered cylinder row. Sumner et al. (2000) identified the flow pattern boundaries for two staggered cylinders. According to the map of Sumner et al. (2000) the flow pattern of the case of this coiled wire is located on the boundary line between "synchronized vortex shedding" (SVS) and "vortex impingement"(VI), in the Reynolds number range 850–1900. In the case of this coiled wire (Fig. 17), the Reynolds number is about 8571. It is difficult to understand the vortex behavior using only COP data. We could not confirm whether the vortex impinges or not in this case. In the literature the Strouhal number for

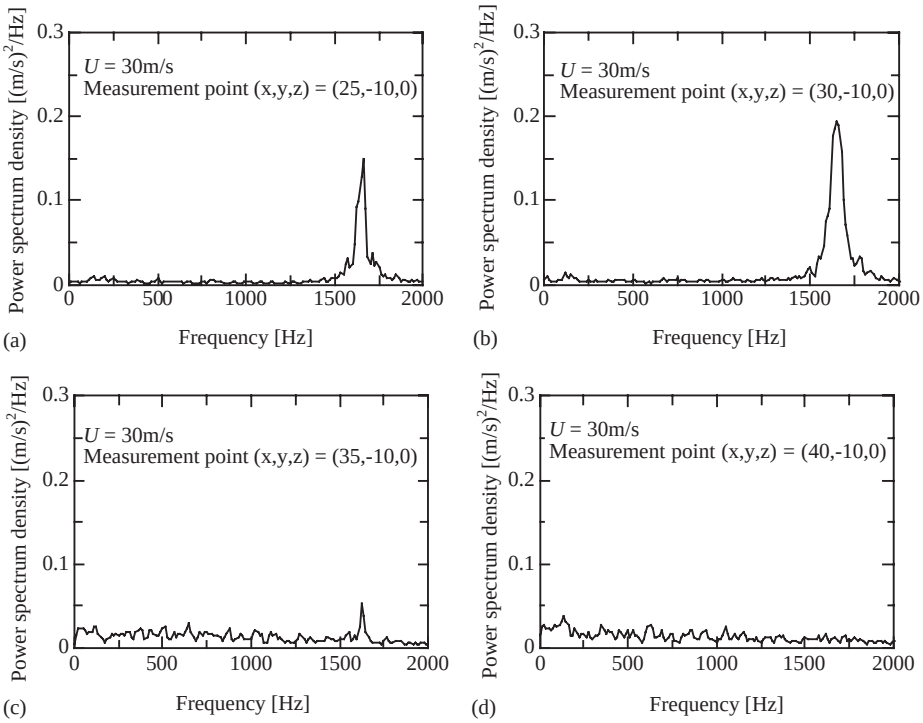

Fig. 18. Power spectrum of velocity fluctuations. (a) The measurement point $(x, y, z) = (25, -10, 0)$ and (b) (30,−10,0), (c) (35,−10,0), (d) (40,−10,0).

this coiled wire case is about 0.2; but the measured Strouhal number of the present coiled wire is 0.22, i.e., it is slightly higher than that in the literature. The reason for this difference could not be explained at present. Explanations of these unknown points are the next goal for us.

5. Conclusions

In this paper, the characteristics of the aerodynamic sound generated by coiled wires have been examined. Moreover, concerning the correlation between the aerodynamic sound and the velocity fluctuations in the wake behind the coiled wire is researched by using the method of measuring $\psi_{nv(fl-fu)}$ (the band overall value of COP). The results obtained may be summarized as follows.

1. When s/d is greater than 1, the spectrum of the aerodynamic sound generated by the coiled wire has a prominent peak.
2. The directivity pattern of the aerodynamic sound source due to the coiled wire differs from the Aeolian sound source due to a single cylinder.
3. Using the method of measuring $\psi_{nv}(f_l - f_u)$, it is possible to clarify the distribution of the strong correlation between the velocity fluctuation in the wake and the aerodynamic sound generated by the coiled wire.
4. The aerodynamic sound generated by the coiled wire is dominated by the vortex shedding from the upstream side arc part of the coiled wire.

Acknowledgements

This research has been supported by a research grant from Research Fellowships of the Japan Society for the Promotion of Science for Young Scientists.

References

Iida, A., Otaguro, T., Yakano, Y., Fujita, H., 1998. Visualization of aerodynamic sound source in a turbulent wake. Proceedings of the INTER-NOISE 98, Paper No. 38.

Bendat, J.S., Piersol, A.G., 1980. Engineering Applications of Correlation and Spectral Analysis. Wiley, New York.

Sumner, D., Price, S.J., Païdoussis, M.P., 2000. Flow-pattern identification for two staggered circular cylinders in cross-flow. Journal of Fluid Mechanics 411, 263–303.

Fujita, H., Shiraishi, J., Kurita, T., Maruta, Y., Yamada, S., 1996. Acoustical and aerodynamic characteristics of end plate materials for two-dimensional models in low noise wind tunnel experiments. Proceedings of the INTER-NOISE 96, pp. 1227–1230.

Fujita, H., Yamada, S., Maruta, Y., Maki, H., 1997. Control of aerodynamic noise generated from two-dimensional models. Proceedings of the INTER-NOISE 97, pp. 371–374.

Mochizuki, O., Kiya, M., Suzuki, T., Arai, T., 1994. Vortex-shedding sound generated by two circular cylinders arranged in tandem. Transactions of the Japan Society of Mechanical Engineers 60–578, 1–7 (in Japanese).